Journal of Thermal Analysis and Calorimetry (2020) 139:649–659
https://doi.org/10.1007/s10973-019-08401-7

Design of heat exchanger with combined turbulator

Truong Khang Nguyen[1,2] · M. Sheikholeslami[3] · M. Jafaryar[4] · Ahmad Shafee[5] · Zhixiong Li[6,7] · Kotturu V. V. Chandra Mouli[8] · I. Tlili[8]

Received: 7 January 2019 / Accepted: 20 May 2019 / Published online: 29 May 2019

Abstract

In this article, influence of inserting new turbulator on resistance and heat transfer behaviors of a pipe has been analyzed. This kind of turbulator can be utilized for retrofit applications. Turbulent nanofluid flow is imposed. Homogenous approach for nanofluid and k–ε approach for turbulent modeling were involved. Contours are presented for different inlet velocity and pitch ratio. Results indicated that the lower the pitch ratio, the better is the temperature gradient. Nanofluid transfers more heat with decline of pitch ratio because of lower generation of longitudinal disturbance. As inlet velocity augments and pitch ratio decreases, nanofluid can scour the wall more easily and heat transfer rate is strengthened.

Keywords Heat exchanger · New turbulator · Nanomaterial · Turbulent

List of symbols

Pr Prandtl number
f Darcy friction factor
p Pressure
P Pitch ratio
Re Reynolds number
T Fluid temperature
Nu Nusselt number
L_t Test section length

Greek symbols

ρ Density
ϕ Concentration of nanoparticles
μ Dynamic viscosity of nanofluid
α Thermal diffusivity

Subscripts

s Solid
nf Working fluid
f Water
s Particles
p Smooth

Introduction

For heat exchange tools, common carrier fluids such as oil and water have been utilized. Reducing the size of heat exchanger makes its thermal performance to augment. One way can help us to design smaller equipment is utilizing nanoparticles and dispersing them into common testing

✉ Zhixiong Li
zhixiongli.cumt@gmail.com

Truong Khang Nguyen
nguyentruongkhang@tdtu.edu.vn

1 Division of Computational Physics, Institute for Computational Science, Ton Duc Thang University, Ho Chi Minh City, Vietnam

2 Faculty of Electrical and Electronics Engineering, Ton Duc Thang University, Ho Chi Minh City, Vietnam

3 Department of Mechanical Engineering, Babol Noshirvani University of Technology, Babol, Islamic Republic of Iran

4 MR CFD LLC, No 49, Gakhokidze Street, Isani-Samgori District, Tbilisi, Georgia

5 Applied Science Department, College of Technological Studies, Public Authority of Applied Education and Training, Shuwaikh, Kuwait

6 School of Engineering, Ocean University of China, Qingdao 266110, China

7 School of Mechanical, Materials, Mechatronic and Biomedical Engineering, University of Wollongong, Wollongong, NSW 2522, Australia

8 Department of Mechanical and Industrial Engineering, College of Engineering, Majmaah University, Al-Majmaah 11952, Saudi Arabia

fluids. The first researcher who introduced nanofluid was Choi [1]. After publishing such proposal, other researcher tried to develop various kinds of nanomaterial for various uses [2–8].

Wang et al. [9] reported about 70% augmentation in thermal efficiency by utilizing CNT nanoparticle with concentration of 0.05%. Alumina working fluid has been utilized by Wen and Ding [10] inside a pipe with uniform heat flux. They examined that concentration of nanoparticle has direct relation with temperature gradient. They concerned the Brownian motion impact and found that thinner boundary layer can be obtained in greater fraction of nanofluid. Sheikholeslami et al. [11] imposed new configuration of swirl flow insert inside a pipe. They inferred that entropy generation acts against Nusselt number. Nadeem et al. [12] utilized nanomaterial along a curved plate. They imposed variable viscosity. Animasaun et al. [13] observed the migration of nanoparticles because of applying magnetic force. They reported the influence of thermoelectric effect on copper oxide–water nanofluid. Sheikholeslami et al. [14] explored mesoscopic simulation for 3D laminar nanofluid MHD flow within a porous domain. Researchers developed nanofluid simulation in the presence of various external forces [15–21]. Sheikholeslami et al. [22] tried to find the treatment of NEPCM in the existence of V-shaped fins during solidification. Saleem et al. [23] demonstrated the hydrothermal performance of radiative nanomaterial in appearance of heat sources. Various turbulent approaches have been tested by Sekrani et al. [24] to model the alumina nanofluid behavior inside a pipe with uniform heat flux. Range of *Re* is 3000–20,000.

Migration of SiO_2 nanoparticles inside a solar collector has been scrutinized by Yan et al. [25]. They inferred that k_{nf} enhances with rise of fraction of nanofluid. Michael and Iniyan [26] scrutinized the impact of dispersing copper oxide on convective flow. They concluded that efficiency enhances about 6.3% by involving 0.05% of mass fraction. Development of numerical approaches for heat transfer modeling is observable in recent years [27–34]. Gupta et al. [35] examined the application of alumina nanomaterial for solar energy saving. They concluded that mass flow rate has optimum values for both pure and nanofluid testing fluid.

In the current text, influence of complex shape of turbulator on hydrothermal behavior of hybrid nanofluid has been examined. Pitch ratio and Reynolds number are two active parameters, and various contours are reported for various values of them. To simulate this problem, FVM was utilized.

Physical model and explanations

The geometry of current turbulators which are inserted within the pipe with constant heat flux condition is demonstrated in Fig. 1. Main geometric parameters have been listed in the right side of geometry. The domain was divided into three zones with equal length, and the central one is test part and turbulators were situated in that zone. The carrier fluid is water-based nanofluid with hybrid nanoparticles (MWCNT and Fe_3O_4). All details for estimating working fluid were mentioned in previous articles [36, 37]. In Table 1, properties of hybrid nanofluid with concentration of 0.003 have been written [37]. Moreover, an example for grid is presented in Fig. 1. Boundary layer grids over the solid surfaces were involved. Mesh is greatly refined near the walls. Number of layers around solid surface is dependent on turbulent model, because utilized mesh should satisfy the limitation of Y^+. As discussed in the previous publication, k–ε model is the best accurate mode for heat exchangers with twisted tape [38]. So, we proposed this model for the current model. In this publication, ANSYS FLUENT 18.1 is employed for simulation. The convergence criterion should be less than 10^{-5}. All utilized settings are the same as Ref. [39]. No slip conditions have been enforced on all solid walls. Corresponding above explanations the governing equations can be listed as:

$$\frac{\partial (u_i)}{\partial x_i} = 0 \tag{1}$$

$$\frac{\partial}{\partial x_j}\left(\rho_{nf} u_i u_j\right) = -\frac{\partial p}{\partial x_i} + \frac{\partial}{\partial x_j}\left(-\rho_{nf}\overline{u'_j u'_i}\right) + \frac{\partial}{\partial x_j}\left(\left(\frac{\partial u_i}{\partial x_j} + \frac{\partial u_j}{\partial x_i}\right)\mu_{nf}\right) \tag{2}$$

$$\frac{\partial}{\partial x_i}\left(\rho_{nf} T u_i\right) = \frac{\partial}{\partial x_i}\left(\left(\Gamma + \Gamma_t\right)\frac{\partial T}{\partial x_i}\right), \quad \Gamma(=\mu_{nf}/Pr_{nf}), \quad \Gamma_t(=\mu_t/Pr_t) \tag{3}$$

μ_t and $\rho_{nf}\overline{u'_j u'_i}$ re:

$$\mu_t = \frac{1}{\varepsilon} k^2 C_\mu \rho_{nf} \tag{4}$$

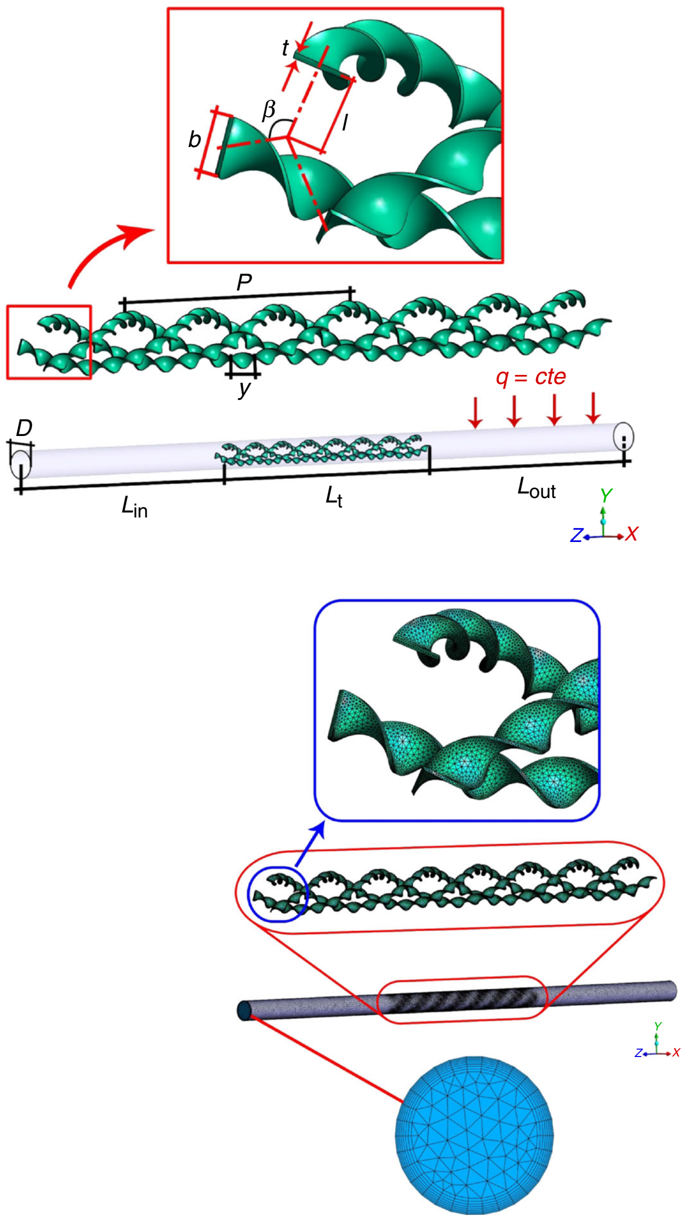

$L_{in} = L_t = L_{out}$	0.5 m
P	0.1 to 0.2 m
y	0.0345 m
D	0.05 m
b	0.01 m
l	0.015 m
t	0.001 m

Fig. 1 Geometry demonstration and sample grid

Table 1 Properties of hybrid nanofluid with concentration of 0.003 [37]

μ/mPa s	1.01
C_p/j kgk^{-1}	4183.99
ρ/kg m^{-3}	1010.04
k/W m k^{-1}	0.6856

$$-\rho_{nf}\overline{u_i'u_j'} = \left(\frac{\partial u_i}{\partial x_j} + \frac{\partial u_j}{\partial x_i}\right)\mu_t - \frac{2}{3}\rho_{nf} k \delta_{ij} - \frac{2}{3}\mu_t \frac{\partial u_k}{\partial x_k}\delta_{ij}. \quad (5)$$

To find k and ε, we have:

$$\frac{\partial}{\partial x_j}\left(\left(\frac{\mu_t}{\sigma_k} + \mu_{nf}\right)\frac{\partial k}{\partial x_j}\right) - \rho_{nf}\varepsilon + G_k = \frac{\partial}{\partial x_i}(u_i \rho_{nf} k),$$
$$G_k = -\rho_{nf}\overline{u_j'u_i'}\frac{\partial u_j}{\partial x_i} \quad (6)$$

$$\frac{\partial}{\partial x_i}(u_i \rho_{nf}\varepsilon) = \frac{\varepsilon}{k} G_k C_{1\varepsilon} - \rho_{nf}\frac{\varepsilon^2}{k} C_{2\varepsilon} + \frac{\partial}{\partial x_j}\left(\left(\frac{\mu_t}{\sigma_\varepsilon} + \mu_{nf}\right)\frac{\partial \varepsilon}{\partial x_j}\right) \quad (7)$$

$$C_{1\varepsilon} = 1.42, \quad C_\mu = 0.0845, \quad C_{2\varepsilon} = 1.68, \quad Pr_t = 0.85, \quad \sigma_k = 1, \quad \sigma_\varepsilon = 1.3. \quad (8)$$

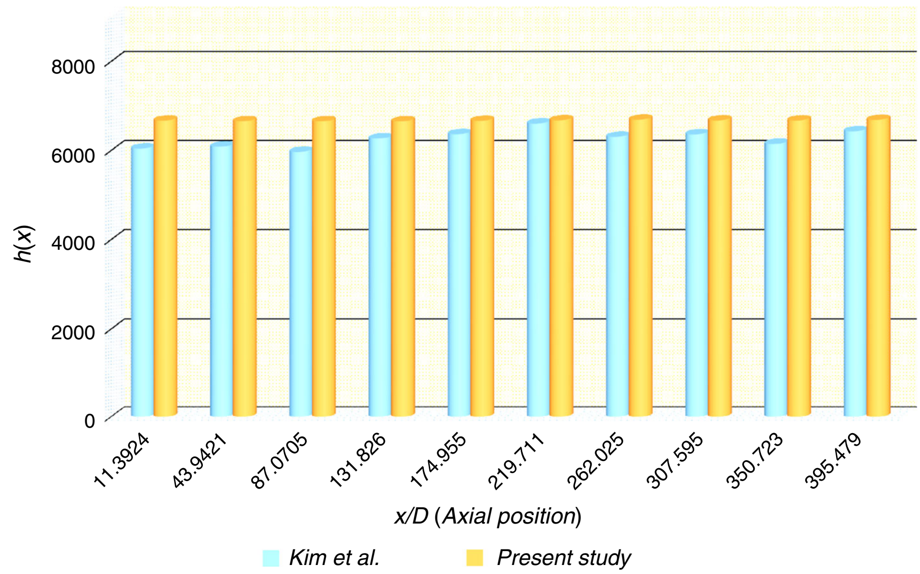

Fig. 2 Verification for h values along the pipe when $\phi = 0.03$ and Re = 6020 [40]

As mentioned, we utilized hybrid nanofluid model as same as Ref. [37] to estimate nanofluid properties.

The inlet and outlet conditions used in the calculation are velocity inlet and pressure outlet:

$$v_{\mathrm{i}} = 0, \quad w_{\mathrm{i}} = cte, \quad u_{\mathrm{i}} = 0, \quad I = 0.16(Re)^{\frac{-1}{8}}, \quad T_{\mathrm{i}} = cte \tag{9}$$

$$\frac{\partial u}{\partial z} = \frac{\partial v}{\partial z} = \frac{\partial T}{\partial z} = \frac{\partial w}{\partial z} = 0. \tag{10}$$

Results and discussion

The numerical study explores the behavior of hybrid nanofluid within a pipe with new type of swirl flow tools which are situated at test section. Homogenous model for nanofluid and k–ε model for turbulent mode have been imposed. We present the contours in three sections A, B and C which are inlet, middle and outlet sections of test section zone.

Before starting simulation, we first examined the validation test. The previous published paper has been selected for comparison in which alumina nanofluid with concentration of 0.03 was testing fluid and Reynolds number is equal to 6020 [40]. Distribution of $h(x)$ is shown in Fig. 2 in which no large deviation can be seen. So, the used code has nice accuracy. Distribution of velocity, streamline, temperature as well as contour of temperature along longitudinal cross section is illustrated in Figs. 3–7. Insertion of turbulator generates longitudinal disturbance. Heat transfer rate has direct relation with irregular disturbance. Greater value of irregular disturbance leads to thinner thermal boundary layer. As pitch ratio declines, more mixing occurs due to greater irregular disturbance. So, nanofluid can scour the wall stronger and heat transfer can be increased. As inlet velocity enhances, the intensity of the swirls produced by turbulator augments considerably, thereby enhancing the heat transfer rate. The weakening of mixing caused by greater pitch ratio reduces the Nusselt number. Greater space of swirl device is in contact with the carrier fluid for lower pitch ratio. So, pressure drop reduces with rise of pitch ratio. Thus, it is necessary to designing turbulator with higher number of evaluations. In addition, it can be inferred that pumping power has direct relationship with temperature gradient.

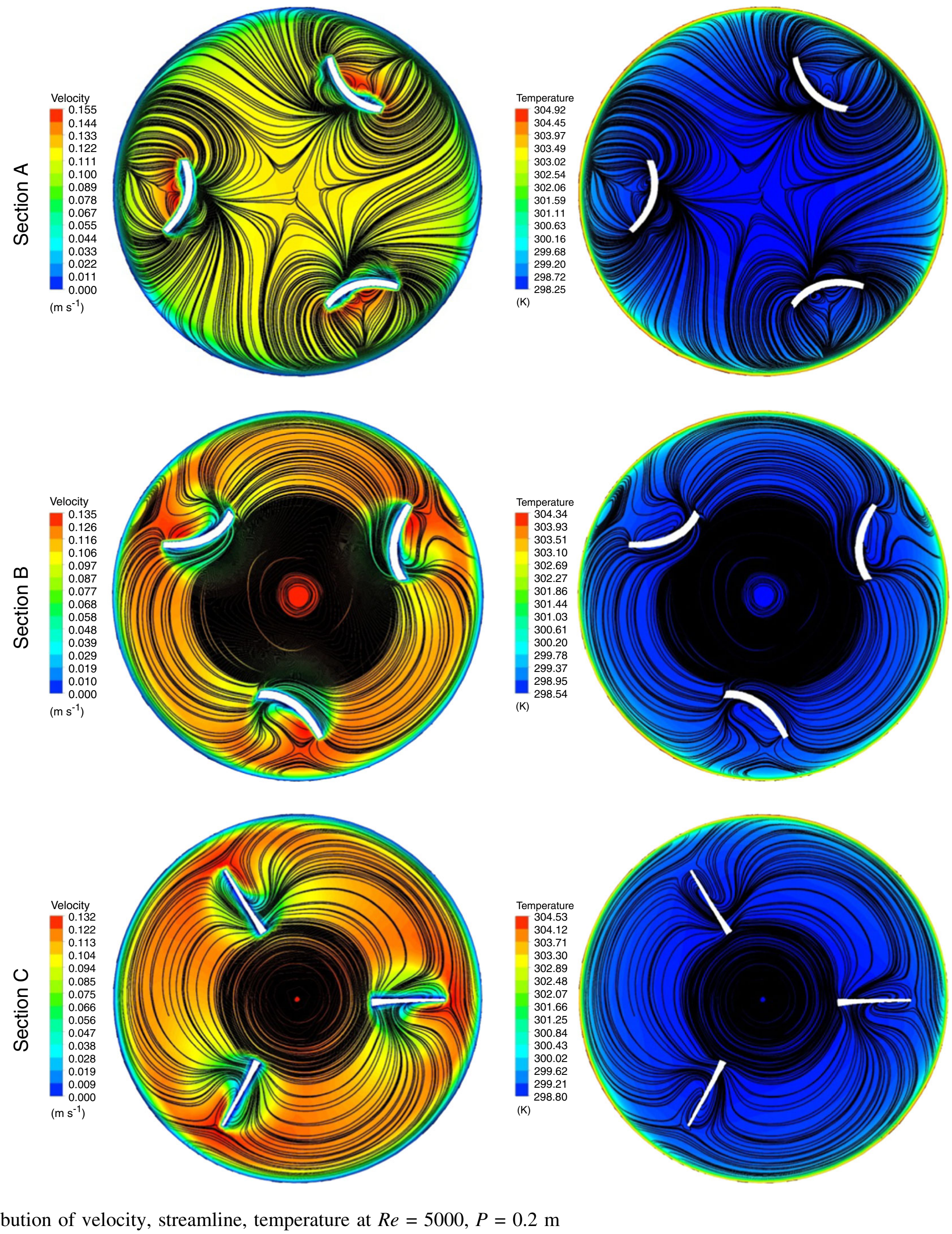

Fig. 3 Distribution of velocity, streamline, temperature at Re = 5000, P = 0.2 m

Variations in ΔP and Nu are presented in Fig. 8. Increasing irregular disturbance makes the pressure drop to enhance. So, ΔP augments with decrease in pitch ratio. Nu demonstrates an enhancing trend with changing Reynolds number, while opposite outputs were reported for pitch ratio. The smaller the pitch ratio, the smaller is the pressure loss.

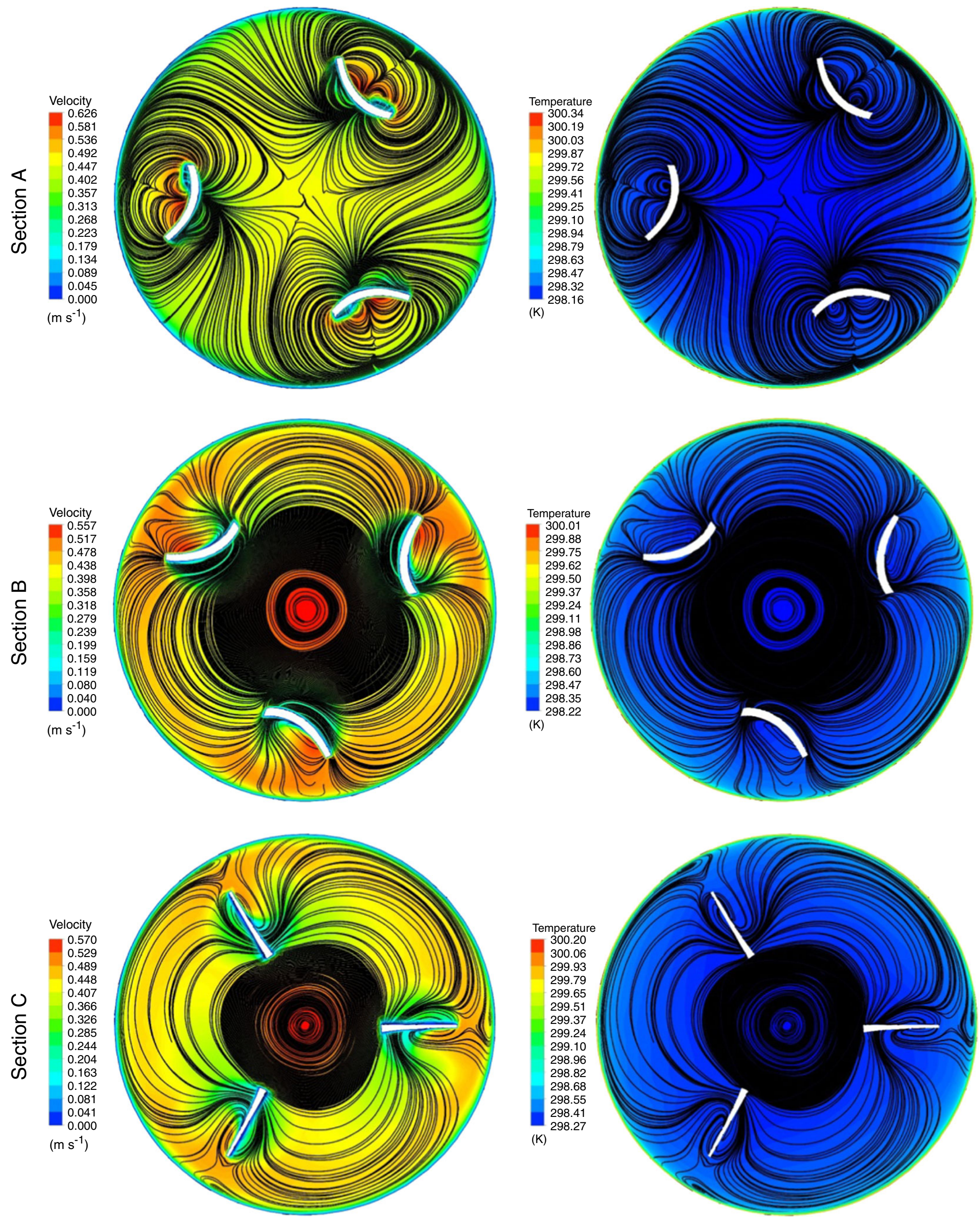

Fig. 4 Distribution of velocity, streamline, temperature at Re = 20,000, P = 0.2 m

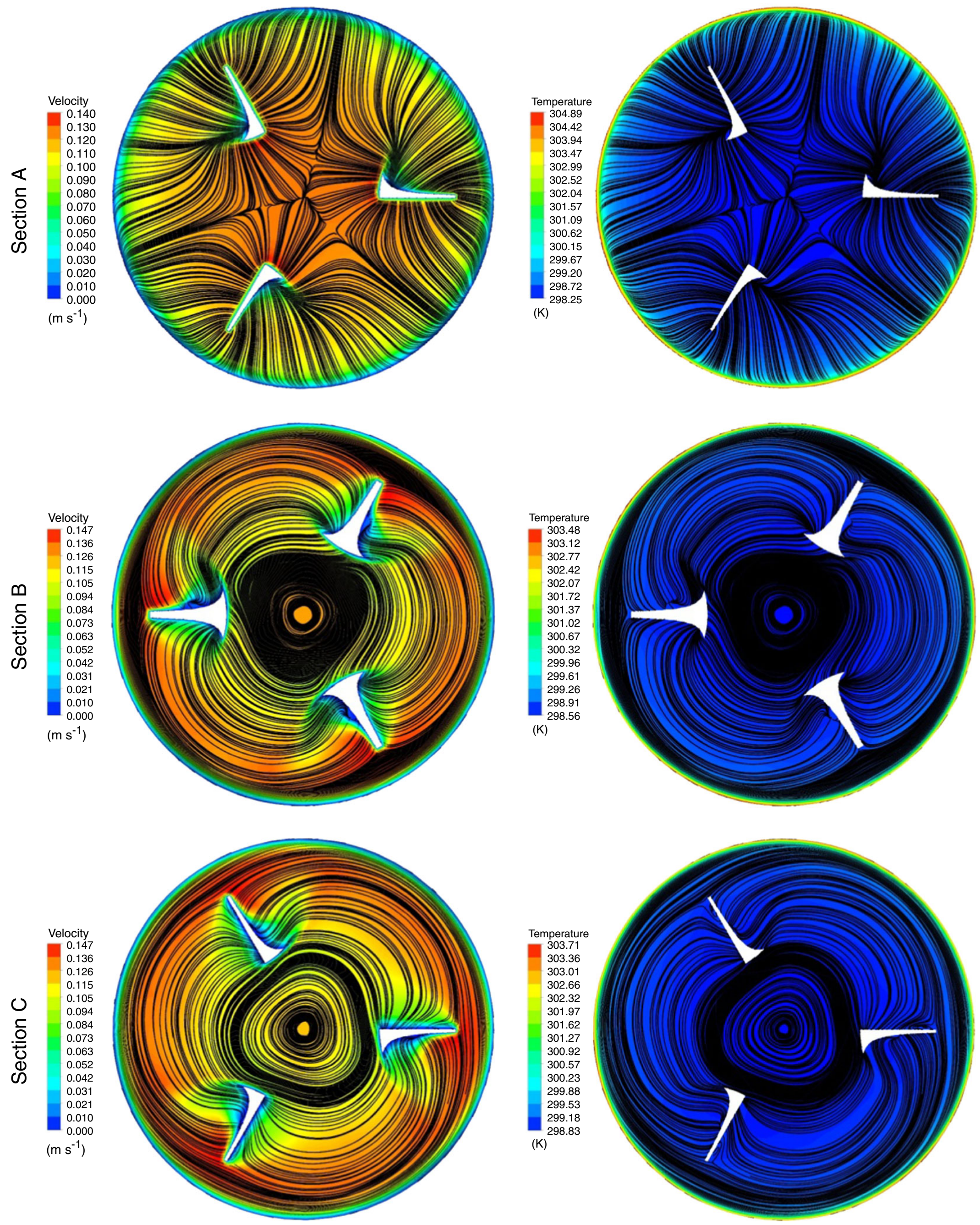

Fig. 5 Distribution of velocity, streamline, temperature at Re = 5000, P = 0.1 m

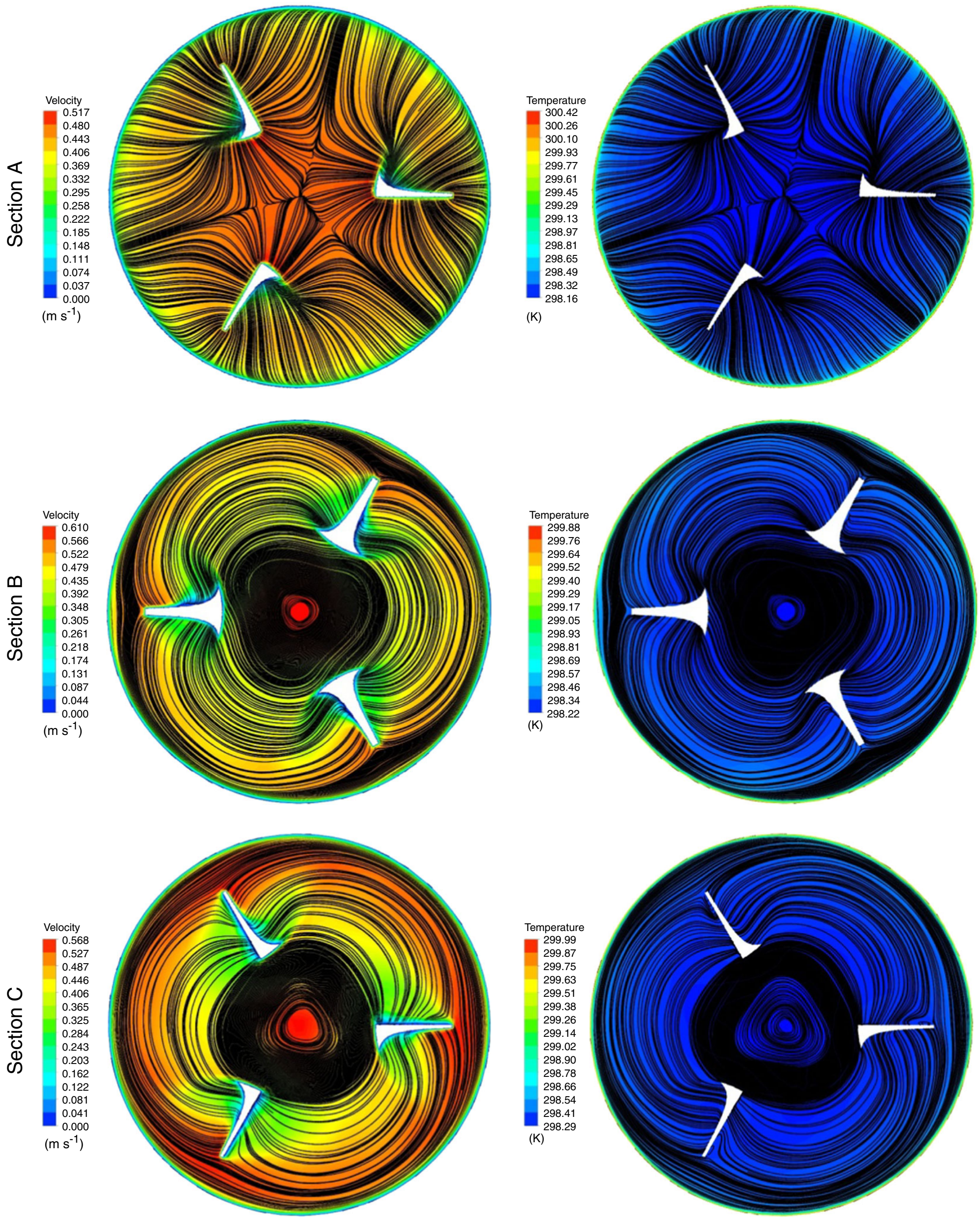

Fig. 6 Distribution of velocity, streamline, temperature at Re = 20,000, P = 0.1 m

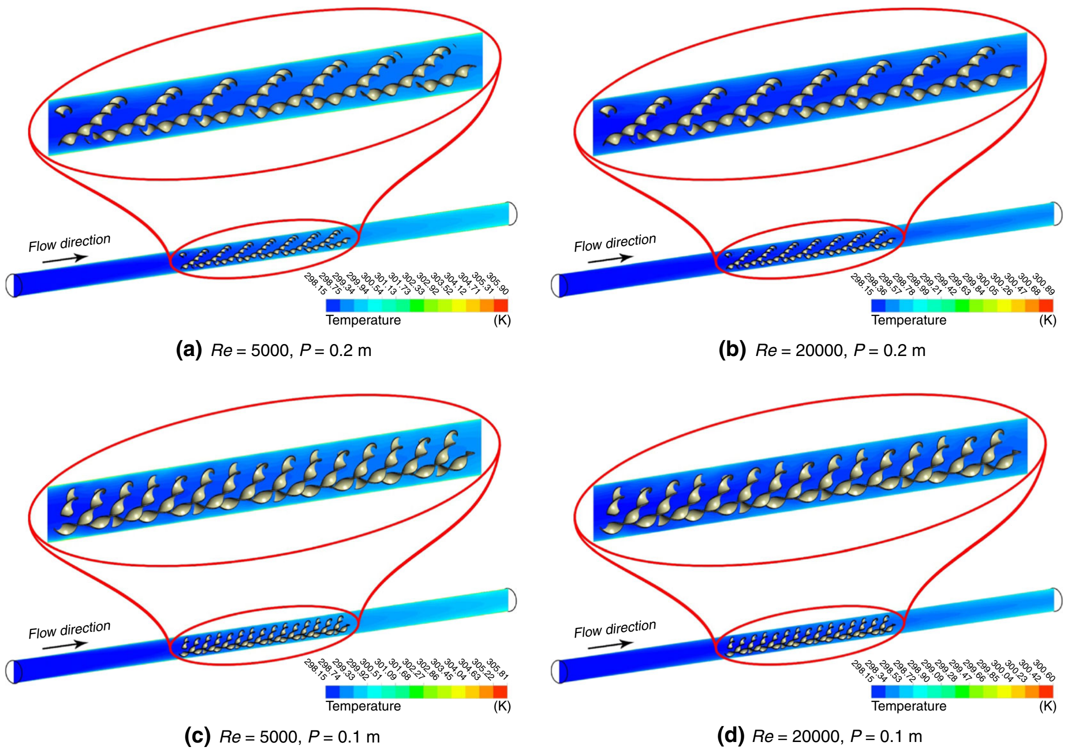

Fig. 7 Contour plot of temperature along cross section for various cases

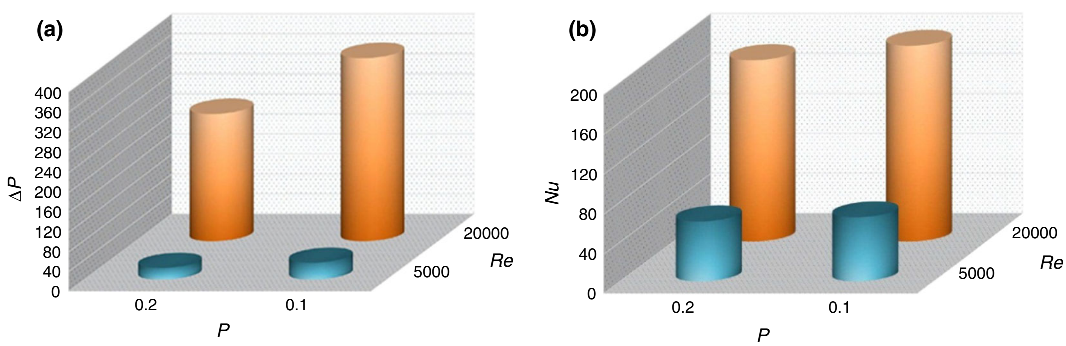

Fig. 8 **a** Pressure drop; **b** Nusselt number for various *Re* and *P*

Conclusions

In the current publication, innovative turbulator is designed and inserted inside the heat exchanger and its influence of efficiency of pipe under turbulent regime condition is simulated. Hybrid nanomaterial moves within the pipe. Turbulators with lower pitch ratio are favorable types of turbulator, which generate the greater turbulent intensity. Thickness of the temperature boundary layer increases when the pitch ratio enhances. Worse heat transfer rate is obtained for lower pitch ratio.

Acknowledgements Dr. Kotturu V. V. Chandra Mouli would like to thank Deanship of Scientific Research at Majmaah University for supporting this work under the Project Number No. 1440-101.

References

1. Choi SUS. Enhancing thermal conductivity of fluids with nanoparticles. In: Developments and applications of non-Newtonian flows FED, vol 231/MDvol. 66. New York: ASME; 1995. pp. 99–105.
2. Sadiq MA, Khan AU, Saleem S, Nadeem S. Numerical simulation of oscillatory oblique stagnation point flow of a magneto micropolar nanofluid. RSC Adv. 2019;9:4751–64.

3. Sheikholeslami M, Jafaryar M, Hedayat M, Shafee A, Li Z, Nguyen TK, Bakouri M. Heat transfer and turbulent simulation of nanomaterial due to compound turbulator including irreversibility analysis. Int J Heat Mass Transf. 2019;137:1290–300.
4. Mamatha Upadhya S, Raju CSK, Mahesha C, Saleem S. Nonlinear unsteady convection on micro and nanofluids with Cattaneo–Christov heat flux. Results Phys. 2018;9:779–86.
5. Sheikholeslami M, Haq RU, Shafee A, Li Z, Elaraki YG, Tlili I. Heat transfer simulation of heat storage unit with nanoparticles and fins through a heat exchanger. Int J Heat Mass Transf. 2019;135:470–8.
6. Shah Z, Islam S, Gul T, Bonyah E, Khan MA. The electrical MHD and hall current impact on micropolar nanofluid flow between rotating parallel plates. Results Phys. 2018;9:1201–14.
7. Sun Z, Shi J, Wu K, Li X. Gas flow behavior through inorganic nanopores in shale considering confinement effect and moisture content. Ind Eng Chem Res. 2018;57:3430–40.
8. Kashyap D, Dass AK. Two-phase lattice Boltzmann simulation of natural convection in a Cu–water nanofluid-filled porous cavity: effects of thermal boundary conditions on heat transfer and entropy generation. Adv Powder Technol. 2018;29(11):2707–24.
9. Wang J, Zhu J, Zhang X, Chen Y. Heat transfer and pressure drop of nanofluids containing carbon nanotubes in laminar flows. Exp Therm Fluid Sci. 2013;44:716–21.
10. Wen D, Ding Y. Experimental investigation into convective heat transfer of nanofluid at the entrance region under laminar flow conditions. Int J Heat Mass Transf. 2004;47(24):5181–8.
11. Sheikholeslami M, Jafaryar M, Shafee A, Li Z, Haq RU. Heat transfer of nanoparticles employing innovative turbulator considering entropy generation. Int J Heat Mass Transf. 2019;136:1233–40.
12. Nadeem S, Ahmed Z, Saleem S. Carbon nanotubes effects in magneto nanofluid flow over a curved stretching surface with variable viscosity. Microsyst Technol. 2018. https://doi.org/10.1007/s00542-018-4232-4.
13. Animasaun IL, Mahanthesh B, Jagun AO, Bankole TD, Sivaraj R, Shah NA, Saleem S. Significance of Lorentz force and thermoelectric on the flow of 29 nm CuO–water nanofluid on an upper horizontal surface of a paraboloid of revolution. J Heat Transfer. 2019;141(2):022402. https://doi.org/10.1115/1.4041971.
14. Sheikholeslami M, Keramati H, Shafee A, Li Z, Alawad OA, Tlili I. Nanofluid MHD forced convection heat transfer around the elliptic obstacle inside a permeable lid drive 3D enclosure considering lattice Boltzmann method. Phys A Stat Mech Appl. 2019;523:87–104.
15. Alkanhal TA, Sheikholeslami M, Arabkoohsar A, Haq RU, Shafee A, Li Z, Tlili I. Simulation of convection heat transfer of magnetic nanoparticles including entropy generation using CVFEM. Int J Heat Mass Transf. 2019;136:146–56.
16. Sheikholeslami M, Arabkoohsar A, Khan I, Shafee A, Li Z. Impact of Lorentz forces on Fe_3O_4–water ferrofluid entropy and exergy treatment within a permeable semi annulus. J Clean Prod. 2019;221:885–98.
17. Roy NC, Rahman T, Hossain MA, Gorla RSR. Boundary-layer characteristics of compressible flow past a heated cylinder with viscous dissipation. J Thermophys Heat Transf. 2019;33(1):10–22. https://doi.org/10.2514/1.t5400.
18. Hammed H, Haneef M, Shah Z, Islam S, Khan W, Muhammad S. The combined magneto hydrodynamic and electric field effect on an unsteady Maxwell nanofluid flow over a stretching surface under the influence of variable heat and thermal radiation. Appl Sci. 2018;8:160. https://doi.org/10.3390/app8020160.
19. Rashidi S, Mahian O, Languri EM. Applications of nanofluids in condensing and evaporating systems. J Therm Anal Calorim. 2018;131:2027–39.
20. Sheikholeslami M, Mahian O. Enhancement of PCM solidification using inorganic nanoparticles and an external magnetic field with application in energy storage systems. J Clean Prod. 2019;215:963–77.
21. Maleki H, Safaei MR, Alrashed AAA, Kasaeian A. Flow and heat transfer in non-Newtonian nanofluids over porous surfaces. J Therm Anal Calorim. 2018. https://doi.org/10.1007/s10973-018-7277-9.
22. Sheikholeslami M, Haq RU, Shafee A, Li Z. Heat transfer behavior of nanoparticle enhanced PCM solidification through an enclosure with V shaped fins. Int J Heat Mass Transf. 2019;130:1322–42.
23. Saleem S, Nadeem S, Rashidi MM, Raju CSK. An optimal analysis of radiated nanomaterial flow with viscous dissipation and heat source. Microsyst Technol. 2019;25:683–9.
24. Sekrani G, Poncet S, Proulx P. Modeling of convective turbulent heat transfer of water-based Al_2O_3 nanofluids in an uniformly heated pipe. Chem Eng Sci. 2018;176:205–19.
25. Yan S, Wang F, Shi Z, Tian R. Heat transfer property of SiO_2/water nanofluid flow inside solar collector vacuum tubes. Appl Therm Eng. 2017;118:385–91.
26. Michael JJ, Iniyan S. Performance of copper oxide/water nanofluid in a flat plate solar water heater under natural and forced circulations. Energy Convers Manag. 2015;95:160–9.
27. Li Z, Saleem S, Shafee A, Chamkha AJ, Du S. Analytical investigation of nanoparticle migration in a duct considering thermal radiation. J Therm Anal Calorim. 2018. https://doi.org/10.1007/s10973-018-7517-z.
28. Sheikholeslami M. New computational approach for exergy and entropy analysis of nanofluid under the impact of Lorentz force through a porous media. Comput Methods Appl Mech Eng. 2019;344:319–33.
29. Sheikholeslami M, Jafaryar M, Shafee A, Li Z. Nanofluid heat transfer and entropy generation through a heat exchanger considering a new turbulator and CuO nanoparticles. J Therm Anal Calorim. 2019;1:1. https://doi.org/10.1007/s10973-018-7866-7.
30. Sun F, Yao Y, Li X, Li G, Miao Y, Han S, Chen Z. Flow simulation of the mixture system of supercritical CO_2 & superheated steam in toe-point injection horizontal wellbores. J Pet Sci Eng. 2018;163:199–210.
31. Rokni HB, Gupta A, Moore JD, McHugh MA, Bamgbaded BA, Gavaises M. Purely predictive method for density, compressibility, and expansivity for hydrocarbon mixtures and diesel and jet fuels up to high temperatures and pressures. Fuel. 2019;236:1377–90.
32. Sun F, Yao Y, Li X, Li G, Liu Q, Han S, Zhou Y. Effect of friction work on key parameters of steam at different state in toe-point injection horizontal wellbores. J Pet Sci Eng. 2018;164:655–62.
33. Sheikholeslami M. Numerical approach for MHD Al_2O_3–water nanofluid transportation inside a permeable medium using innovative computer method. Comput Methods Appl Mech Eng. 2019;344:306–18.
34. Rokni HB, Moore JD, Gupta A, McHugh MA, Gavaises M. Entropy scaling based viscosity predictions for hydrocarbon mixtures and diesel fuels up to extreme conditions. Fuel. 2019;241:1203–13.
35. Gupta HK, Agrawal GD, Mathur J. Investigations for effect of Al_2O_3–H_2O nanofluid flow rate on the efficiency of direct absorption solar collector. Case Stud Therm Eng. 2015;5:70–8.
36. Sundar LS, Singh MK, Sousa ACM. Enhanced heat transfer and friction factor of MWCNT–Fe_3O_4/water hybrid nanofluids. Int Commun Heat Mass Transf. 2014;52(73):83.
37. Sheikholeslami M, Mehryan SAM, Shafee A, Sheremet MA. Variable magnetic forces impact on magnetizable hybrid

nanofluid heat transfer through a circular cavity. J Mol Liq. 2019;277:388–96.
38. Farshad SA, Sheikholeslami M. Nanofluid flow inside a solar collector utilizing twisted tape considering exergy and entropy analysis. Renew Energy. 2019;141:246–58.
39. Sheikholeslami M, Jafaryar M, Li Z. Nanofluid turbulent convective flow in a circular duct with helical turbulators considering CuO nanoparticles. Int J Heat Mass Transf. 2018;124:980–9.
40. Kim D, Kwon Y, Cho Y, Li C, Cheong S, Hwang Y, Lee J, Hong D, Moona S. Convective heat transfer characteristics of nanofluids under laminar and turbulent flow conditions. Curr Appl Phys. 2009;9:119–23.